coatings

MDPI

Article

Study of the Adhesion of Silicate-Based Coating Formulations on a Wood Substrate

Arnaud Maxime Cheumani Yona [1,2,*], Jure Žigon [1], Sebastian Dahle [1] and Marko Petrič [1]

[1] Department of Wood Science and Technology, Biotechnical Faculty, University of Ljubljana, Jamnikarjeva ulica 101, SI-1000 Ljubljana, Slovenia; Jure.Zigon@bf.uni-lj.si (J.Ž.); Sebastian.Dahle@bf.uni-lj.si (S.D.); Marko.Petric@bf.uni-lj.si (M.P.)

[2] Macromolecular Research Team, Faculty of Science, University of Yaoundé 1, P.O. 812 Yaoundé, Cameroon

* Correspondence: ArnaudMaximeCheumani.Yona@bf.uni-lj.si

Abstract: Silicate coatings are environmentally friendly inorganic-based products that have long been used for mineral substrates and protection of steel against corrosion. The development and acceptance of these coatings in the wood sector require some adjustments in formulations or special preparation of the surface to be coated to obtain durable finishes. In this work, the adhesion of various silicate-based formulations to a beech wood substrate (*Fagus sylvatica* L.), was assessed with the main objective to study relevant parameters and potential improvements. Adhesion strength was determined by pull-off and cross-cut tests. Other coating properties such as scratch, impact, and water resistance were also determined. Surface roughness and interface were analyzed using confocal laser scanning microscopy (CLSM) and scanning electron microscopy (SEM), and coating curing was studied by attenuated total reflection-infrared spectroscopy (ATR FTIR). The results showed that adhesion was highly dependent on formulation, penetration of the coatings into wood, and mechanical anchoring. Increasing the content of solid particles in the coating formulations or adding a polyol (glycerol, xylose), which probably acted as a coalescent, considerably decreased the adhesion strength, probably by blocking penetration into the wood by forming aggregates. Adhesion was improved by pre-mineralization of the surface, and substitution of a part of the potassium silicate binder with potassium methyl siliconate reduced the formation of cracks caused by dimensional instability of the wood.

Keywords: coating; silicate; water glass; wood; potassium methyl siliconate; adhesion

check for updates

Citation: Cheumani Yona, A.M.; Žigon, J.; Dahle, S.; Petrič, M. Study of the Adhesion of Silicate-Based Coating Formulations on a Wood Substrate. *Coatings* **2021**, *11*, 61. https://doi.org/10.3390/coatings11010061

Received: 21 December 2020
Accepted: 1 January 2021
Published: 7 January 2021

Publisher's Note: MDPI stays neutral with regard to jurisdictional claims in published maps and institutional affiliations.

Copyright: © 2021 by the authors. Licensee MDPI, Basel, Switzerland. This article is an open access article distributed under the terms and conditions of the Creative Commons Attribution (CC BY) license (https://creativecommons.org/licenses/by/4.0/).

1. Introduction

Wood coatings are used extensively as domestic and industrial finishes for the decoration and surface protection of wood and other wood-based materials. To perform durably, these wood finishing products specifically require good adhesion, flexibility, water resistance, and resistance to other damage-causing parameters (photodegradation, scratching, and impact). The global wood coatings market is currently dominated by organic-based materials. However, there is a growing interest in the development of purely inorganic or inorganic-rich alternative solutions stimulated by new requirements and regulations such as the reduction of volatile organic compounds emissions or the demand for ultraviolet-resistant and fire-retardant products. A large number of research works have been published in recent years on surface coatings of wood by depositing thin layers of various inorganic nanoparticles (e.g., TiO_2, SiO_2, Al_2O_3, ZnO, CuO) or even metallic particles (e.g., Ag, Zn, Cu, Al) using techniques such as sol–gel impregnation, or physical and chemical vapor deposition [1–4]. Silicate-based coating systems are also potential inorganic alternatives that have the added advantage of being formulated for application by any end user with a minimum of experience and for wood renovation.

Silicate coatings consist of water glass (e.g., potassium water glass) or silica sol (e.g., ethyl silicate) or mixtures thereof as the main binder, calcium carbonate, zinc ox-

ide, zinc powder, talc, fine sand extender, and mineral pigments (e.g., TiO_2, Fe_2O_3) [5–7]. Organic additives such as aqueous dispersions of polymers (e.g., styrene-acrylic, styrene-butadiene, polystyrene), thickeners (e.g., hydroxyethyl cellulose), dispersants, and stabilizers can be added to some extent. Silicate coatings are established for concrete, masonry and stone, brick, steel or aluminum and have appeared to be one of the most resilient paints in exterior use. Silicate coatings cure through chemical reactions, which involve formation of strong chemical bonds with inorganic species at the surface of mineral substrates and promote adhesion of the coating to these substrates [5,8]. The higher dimensional stability of mineral substrates compared to wood reduces the stresses exerted on the coatings and favors durability despite the lower flexibility inherent to inorganic materials. Composite primers made of alkyd resins or drying oils modified with mineral particles have been proposed by coating companies (e.g., Keimfarben®, Beeck®) for durable wood silicate coatings. However, scientific literature about their applications for wood and wood products is sparse. To the best of our knowledge, there are no reports in the literature on fundamental studies of the adhesion mechanisms and potential performance improvements of such coatings for wood surfaces. Previous research in this field focused on the fire performances [9,10]. Kumar and co-authors [9] observed that vermiculite-sodium silicate composites coated on wood formed a solid foamy layer and released water molecules that improved the flame retardancy, when exposed to fire. Silicate paints containing hydromagnesite provided the first group of fire resistance for a wooden surface [10]. The authors presented a coating formulation with relatively good adhesion strength values on wood (5–6 MPa), but the research data and optimization work leading to these results were not published (to the best of our knowledge) [10]. Silicate-based geopolymer cements have also been tested for wood coatings, but they are slightly different systems [11–13].

The focus of this work was to fundamentally study the adhesion of silicate coating formulations on wood. Beech wood (*Fagus sylvatica* L.) was used as a substrate. The influence of organic additives such as glycerol, D-(+)-xylose, sucrose and dextrin as well as of the surface pretreatment of the wood are reported. The properties of the fresh liquid formulations were determined by rheological measurements. Adhesion was studied by pull-off (standard ISO 4624-2016 [14]) and cross-cut tests (EN ISO 2409 (1997) [15]), scratch resistance by pencil hardness (standard EN ISO 1518-1 (2000) [16]) and impact resistance according to the standard ISO 4211-4 (1995) [17]. The interface between the coatings and the wood was studied using scanning electron microscopy combined with energy dispersive analysis of X-rays (SEM-EDAX) and the surface roughness was investigated using confocal laser scanning microscopy (CLSM). The resistance of the coating to liquid water was determined and the chemical changes were studied by ATR-FTIR analyses.

2. Materials and Methods

2.1. Materials

European beech wood (*Fagus sylvatica* L.) was used in this study. The dimensions of the plates were approximately 380, 80 and 10 mm for longitudinal, tangential and radial directions, respectively. Potassium hydroxide flakes (90%), lithium hydroxide (98%), silica gel (porosity 60 Å, particle size 63–200 µm) and methyltrimethoxysilane (MTMS 98%) were used to prepare potassium water glass, lithium water glass, and potassium methyl siliconate. The components were mixed with demineralized water to obtain silicate or siliconate solutions with different modulus (molar ratio $SiO_2/(K,Li)_2O$ for water glasses or MTMS/KOH for the siliconate) and solid content of 35%. The prepared water glasses were kept for at least 24 h for maturation before use in formulation of coatings. A precipitated calcium carbonate and a calcium carbonate sample ($\leq$50 µm particle size) were used as fine and coarse powders, respectively, in a 50:50 mass ratio. Glycerol (98%), sucrose ($\geq$99.5%), D-xylose ($\geq$98%), titanium (IV) oxide (99.5%, 21 nm mean particle size) and silicon antifoam (30% in water, emulsion) were used as additives. These chemicals were all purchased from Sigma Aldrich Chemie GmbH, Steinheim, Germany, except the precipitated calcium carbonate (Sigma Aldrich, Darmstadt, Germany), lithium hydroxide (Acrōs organics,

Geel, Belgium) and glycerol (Honeywell, Seelze, Germany). Domemul SA 9263 (styrene-acrylic emulsion, non-volatile matter (39–41%, pH 8–8.5, viscosity at 23 °C 20–350 mPa s) was provided by Helios TBLUS (Količevo, Slovenia). Zinc oxide (≥99%) was obtained from Fluka-Honeywell (Seelze, Germany, talcum (98%) and dextrin were purchased from Roth (Karlsruhe, Germany). The chemicals were all used as received without further purification steps.

2.2. Preparation of the Coatings

The different formulations developed in this study are shown in Table 1. Solid components, styrene-acrylic emulsion, demineralized water and eventually glycerol were weighed in a plastic cup (polypropylene), and premixed with a glass rod. Water glass and silicon antifoam were then added to the mixture and the whole was thoroughly mixed using an IKa® T25 digital ultra-Turrax® (Staufen, Germany) at 3200 rpm for 2 min and 5000 rpm for 3 min. Polyols (glycerol, xylose, dextrin, or sucrose) were added to the formulation as potential plasticizers and adhesion promoters to the wood. A part of potassium water glass was replaced with a potassium methyl siliconate water solution, an organosilicate solution prepared from methyltrimethoxysilane.

Table 1. Recipes for the preparation of different coating formulations.

Samples	Water Glass (g)	Acrylic Resin (g)	$CaCO_3$ (g)	ZnO (g)	Talc (g)	Gly (g)	Xyl (g)	Sucr (g)	Dex (g)	TiO_2 (g)	Water (g)	Silicon (g)
CF1 [a]	35	4	10	5	5	0	0	0	0	0	4	0.2
CF2 [a]	35	4	10	5	5	4	0	0	0	0	4	0.2
CF3 [a]	35	4	10	5	5	0	0	4	0	0	4	0.2
CF4 [a]	35	4	10	5	5	0	4	0	0	0	4	0.2
CF5 [a]	35	4	10	5	5	0	0	0	4	0	4	0.2
CF6 [a]	35	5	30	10	5	0	0	0	0	0	15	0.2
CF7 [a]	35	4	10	5	5	0	0	0	0	5	20	0.2
CF8 [b]	35	4	10	5	5	0	0	0	0	0	4	0.2
CF9 [c]	35	4	10	5	5	0	0	0	0	0	4	0.2
CF10 [d]	35	4	10	5	5	0	0	0	0	0	4	0.2
CF11 [e]	35	4	10	5	5	0	0	0	0	0	4	0.2
CF12 [f]	35	4	10	5	5	0	0	0	0	0	4	0.2

Potassium water glass: (a) module 3.2, (b) module 0.5, (c) module 1.5, (d) module 2.5, (e) lithium silicate module 3.2, and (f) potassium silicate module 3.2 + potassium methyl siliconate module 3.2 75:25 wt.%. Gly: glycerol, Xyl: D-(+)-xylose, Sucr: Sucrose and Dex: Dextrin.

2.3. Rheological Measurements

Rheological properties are important parameters that determine the application and penetration of a coating formulation into a substrate (wood). Rheological measurements of the fresh coating formulations were carried out with an ARES G2 rheometer (TA instruments, New Castle, DE, USA) using two plate parallel geometry. Both plates were 25 mm in diameter, and the gap was fixed between 0.9 and 1 mm. Flow ramp tests were performed at a shear rate from 0 to 1000 s^{-1} at a temperature of 25 °C controlled by an air flow. Three replicates were performed for each sample and the results are mean values of the replicates.

2.4. Application of Coatings on Wood Substrate

The coatings were applied to the longitudinal tangential surface. The surface was sanded with sandpaper 120-grit and dusted off with compressed air. The coatings were applied manually using a coating applicator with a 240 µm wet film thickness outflow at a movement speed of approximately 30 $mm \cdot s^{-1}$. The coated substrates were stored under ambient conditions (temperature (23 ± 3) °C and (50 ± 5)% relative humidity) for two weeks for drying and curing prior to characterization. The coating layers dried within a few hours, but the curing and development of resistances of such reactive inorganic materials required more time for silicification and reactions of silicates with mineral additives.

2.5. Pretreatment of the Wood Samples

Pre-mineralized wood samples were also used as substrates. The pretreatment was carried out by a double impregnation process as proposed by many authors including a silicification step and a curing step to produce insoluble silica [18–20]. Beech wood samples were dipped in a 10 wt.% potassium silicate solutions (module 3.2) for 2 h and dried for 24 h under ambient conditions. They were then dipped again in a 5 wt.% boric acid or 5 wt.% sodium bicarbonate solution for 2 h. Finally, the samples were dried under ambient conditions for 24 h and further in an oven at 105 °C for 24 h. The treated samples were cooled down and kept under ambient conditions for one weak to allow moisture equilibrium before being used for coating experiments.

2.6. Characterization of the Samples

2.6.1. Pull-Off Adhesion Test of the Samples

Pull-off adhesion tests were carried out according to the standard ISO 4624-2016 [14]. Aluminum dollies (20 mm) were glued on the surface of the coatings using a 2-component polyurethane adhesive and allowed to cure for 24 h. The coating around the dollies was carefully cleaned down to the substrate to isolate the glued zone from the rest of the coating layer. The tensile stress (adhesion strength) applied to peel off the coating from wood surface was measured by using a Defelsko Positest® Adhesion tester (Defelsko instruments corporation, Ogdensburg, NY, USA). In general, two types of failure are distinguished: If less than 40% of the coating layer remained on the substrate, the failure is considered adhesive and the measured strength is representative to the adhesion of the coating with the substrate. Otherwise, the failure is regarded as a cohesive type (cohesion of the coating). Three replicates were performed for each sample and the results are mean values of the replicates.

2.6.2. Cross-Cut Analysis of the Samples

The adhesion of the coatings to the wood substrate was also assessed by cross-cut tests carried out according to EN ISO 2409 (1997) [15]. The coatings were cut approximately at 45° to the grain direction using a 2 mm normalized cutting tool. The two series of parallel cuts were crossed at an angle of 90° to obtain a pattern of squares. The sample was brushed and carefully examined using a lighter magnifier (2.5×) and rate based on the step classification given by the standard EN ISO 2409 (1997) [18]. Three replicates were performed for each sample.

2.6.3. Scratch Resistance of the Samples

The scratch resistance was determined according to the standard EN ISO 1518-1 (2000) [16]. The scratching needle with a hard hemispherical tip (tungsten carbide) of 1 mm diameter was drawn across the surface of the coated test specimen at a constant speed of 30–440 $mm \cdot s^{-1}$ perpendicular to the grain direction. Scratching was performed on different points of the coated wood specimens with increasing load on the scratch needle, until the coating cracked or the scratch was wider than 0.5 mm. The force level in N, which produced such a damage, is defined as a critical scratch, and this represents the scratch resistance.

2.6.4. Resistance to Impact of the Samples

The resistance to impact was determined using the standard method ISO 4211-4 (1995) [17]. A steel cylinder of (500 ± 5) g was placed at different heights for free fall onto a steel ball (diameter 14 mm) placed on the surface of the coating. After impact, the surface was examined with a magnifier (10×) and the diameter of the hole left at the surface of the coating was measured. The impact resistance of the coating was evaluated using numerical grades according to the standard. Three replicates were performed for each sample and drop height.

2.6.5. ATR-FTIR of the Samples

Attenuated total reflection-infrared spectroscopy (ATR FTIR) measurements of water glass, fresh silicate formulation and cured coating layers were performed using a Perkin Elmer Spectrum Two (PerkinElmer Inc., Waltham, MA, USA) ATR FTIR spectrometer, with a $LiTaO_3$ detector in the absorbance mode. The spectra were corrected for background noise and 16 scans per sample were collected at a wavelength from 400 to 4000 cm^{-1} at a resolution of 0.5 cm^{-1}.

2.6.6. SEM-EDAX of the Samples

The interface between the wood and the coating layer was examined with Scanning Electron Microscopy (SEM) and Energy-Dispersive Analysis of X-rays (EDAX). The micrographs were taken at a 20 kV voltage and a pressure of 50 Pa using a large field (LFD) detector in a FEI Quanta 250 SEM microscope (FEI Company, Hillsboro, OR, USA) at working distances between 7 and 11 mm under magnification by 300×. The interface and EDAX analyses were performed on fracture surfaces (obtained by splitting the coated wood samples in the longitudinal direction) to minimize the effect of polishing and particle dispersions of a cut-off saw.

2.6.7. Confocal Laser Scanning Microscopy Analyses of the Samples

The surface roughness of the coatings were studied using a Confocal Laser Scanning Microscope (CLSM) Olympus LEXT OLS5000 (Olympus Corporation, Tokyo, Japan) with the following objectives: MPLFLN5× (numerical aperture 0.15, working distance 20 mm). The microscope is equipped with a 405 nm violet laser, which enables a lateral resolution of down to 0.12 μm.

2.6.8. Water Absorption Measurements

The samples of 10 cm × 5.5 cm in size were cut from coated wood and used for water absorption tests. The tests were performed according to EN 927-5 [21] with modification (different sample sizes, no pre-conditioning). The uncoated surfaces were covered with a waterproof epoxy-based coating (Eplor HB, Color, Medvode, Slovenia). Each test specimen was exposed to demineralized water (300 mL) floating on the surface of the water with the investigated coated side facing down. The mass increase associated to water uptake was followed for 72 h. Two to three replicates were performed for each sample and the results are averages of the replicates.

3. Results and Discussion

3.1. Coating Performances

Pull-off adhesion, cross-cut, scratch and resistance to impact of the different coatings applied on beech wood are shown in Table 2.

Adhesion is an important coating parameter that defines the resistance of a coating to detachment from the substrate and is related to the quality of the coating, the physicochemical and mechanical interactions with the surface, and the degree of preparation of the surface before painting [22]. The failure mode after the pull-off test was mainly of the adhesive type, so the values in Table 1 actually reflect the adhesion strength of the coatings on wood. From the results, it can be seen that adhesion strength was significantly dependent on the formulation. Pull-off adhesion strengths comparable to the adhesion of some commercial organic-based coatings were obtained with CF1, CF7 and CF10–CF12. Adhesion strength values reported in the literature for wood coatings generally range from 2 to 5 MPa, but can reach up to 10 MPa for high performance coatings [23–25]. Based on observations of six polyurethane coatings, Oblak and co-authors [26] suggested a minimum acceptable adhesion value of 2.5 MPa for wood, and more than 5 MPa for excellent adhesion. It should be noted that this grade is applicable for organic-based coatings that are film-forming and flexible, and different values could be required for inorganic coatings. The cross-cut results are in line with the classes of adhesion obtained by pull-off tests.

The best result according to the EN ISO 2409 rate was 1, which corresponds to the cross-cut area with small flakes of coatings detached at the cutting intersections, as shown in Figure 1. An increase in rate is related to a decrease in adhesion and more detachment of the coatings as observed with CF4 (Rate 3).

Table 2. Adhesion strength, scratch resistance, and impact resistance of the coating formulations after two weeks of curing under ambient conditions (23 ± 3 °C and (50 ± 5)% relative humidity).

Coating Formulation	Pull-Off Adhesion Strength (MPa) #	Assessment of the Cross-Cut Test (2 mm)	Scratch Resistance (N)	Assessment of the Impact Test *	
				100 mm	400 mm
CF1	2.68 (0.33)	1	6	4 (4.5)	3 (6.3)
CF2	1.44 (0.40)	3	5	3.5 (5.2)	2.5 (6.7)
CF3	1.72 (0.08)	2	6	4 (4.5)	3 (6.3)
CF4	1.21 (0.11)	3	4	3 (5.8)	2.5 (6.8)
CF5	2.25 (0.08)	1	5	4 (4.2)	3 (6.6)
CF6	1.07 (0.13)	5	2	4 (5.8)	2.5 (7.0)
CF7	2.22 (0.06)	1	3	4 (3.5)	2 (6.3)
CF8	0.84 (0.15)	4	2	2.5 (4.5)	2 (6.1)
CF9	0.95 (0.08)	4	3	2.5 (4.8)	2 (7.0)
CF10	2.65 (0.46)	2	5	4 (4.0)	2.5 (7.1)
CF11	2.71 (0.37)	2	4	4 (4.8)	3 (6.3)
CF12	2.65 (0.22)	1	5	4 (4.6)	3 (6.5)

Standard deviation in the parentheses. * 100 and 400 mm is the drop height and values in parentheses the diameter of the crater caused by the impact.

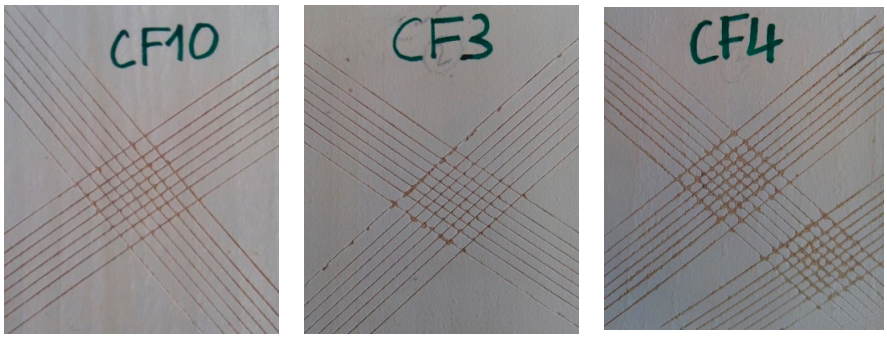

Cross cut-rate 1. **Cross cut-rate 2.** **Cross cut-rate 3.**

Figure 1. Cross-cut adhesion of CF3, CF4 and CF10.

Rate 1 is generally well accepted for commercial organic coatings. Relatively poor adhesion values were measured for the high solid content (CF6) formulation and for formulations with added glycerol, xylose and sucrose (pull-off adhesion lower than 2 MPa and cross-cut results of 2 to 5). The adhesion was higher with dextrin (CF5) than with other sugars and glycerol. The decrease of the modulus of water glass to 1.5 and 0.5 considerably reduced the adhesion of the coatings (CF8 and CF9). The scratch resistance and impact resistance measured with these formulations were also lower, suggesting that the failure was not only at the adhesion level but also on the cohesion and curing state of the coatings. The polymerization degree of silicates in water glass solution decreases with the modulus [5,8], it is probable that low molecular weight silicates are unable to form high strength compounds with the mineral additives (calcium carbonate, zinc oxide or talc). However, the reaction of water glass of low module (around to 0.5) with aluminosilicate compounds such as kaolin, metakaolin or activated fly ash has been demonstrated in the formation of high mechanical strength geopolymer cement binders [11–13]. CF12 showed that potassium water glass can be substituted with potassium methyl siliconate without a considerable loss of performance of the coatings.

The coatings showed acceptable resistance to scratch for some formulations. For comparison, the scratch resistances of cellulose nitrate lacquer, polyurethane, and various wood

varnishes were reported between 1.5 and 4 N [27]. The coatings could withstand impact tests up to a drop height of 400 mm (corresponding to an impact energy of 2 J) without being severely destroyed. Impact holes with increasing diameter were observed, but no cracking and detachment of the coatings.

3.2. Adhesion Mechanisms

The adhesion was studied by interfacial observations. The interface between wood and coatings was analyzed using SEM coupled with EDAX. Four coating formulations were selected for these analyses based on their different level of adhesion strengths and the results are shown in Figure 2.

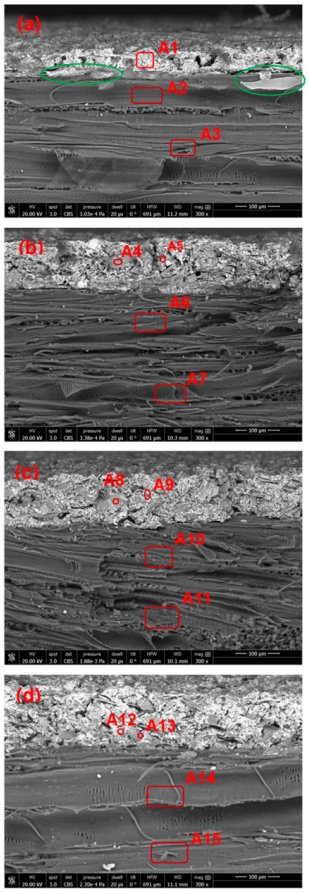

EDXA of area A1, A 2, and A3

Element	A1	A2	A3
CK	29.0	44.3	54.7
OK	41.2	44.0	43.1
MgK	1.5	/	/
SiK	8.7	/	/
SrL	1.8	/	/
KK	2.4	11.7	2.1
CaK	9.8	/	/
ZnK	5.6	/	/

EDXA of area A4, A5, A6 and A7

Element	A4	A5	A6	A7
CK	8.2	37.9	54.2	45.1
OK	50.9	36.7	41.1	45.7
NaK	1.6	1.2	/	/
MgK	17.2	2.1	/	/
SiK	23.7	6.5	0.4	/
KK	/	1.6	4.2	9.2
CaK	/	0.7	/	/
ZnL	/	13.4	/	/

EDXA of area A8, A 9, A10, and A11

Element	A8	A9	A10	A11
CK	29.6	24.4	49.8	50.9
OK	40.1	51.6	47.2	46.8
NaK	2.5	/	/	/
MgK	0.8	1.6	/	/
SiK	8.1	5.4	1.3	/
KK	4.4	2.3	1.7	2.3
CaK	1.7	6.8	/	/
ZnL	12.8	5.4	/	/

EDXA of area A12, A 13, A14, and A15

Element	A12	A13	A14	A15
CK	19.4	20.2	54.2	54.9
OK	34.2	53.0	44.7	45.1
NaK	4.3	1.7	/	/
MgK	1.7	11.3	/	/
ZnL	25.5	/	/	/
SiK	4.9	13.1	1.1	/
CaK	9.0	0.6	/	/
SrL	1.0	/	/	/

Figure 2. SEM-Energy-Dispersive Analysis of X-rays (EDAX) interfacial analyses of beech wood coated with (**a**) CF1 (**b**) CF2 (**c**) CF3 and (**d**) CF11.

The micrograph of CF1 clearly showed the penetration of the coating into the wood structure. The cured coatings (white area in the image of CF1 with green encirclements) can be observed in a few microns into the wood structure. The other white particles observed throughout the wood structure were attributed to the detachment and dispersion of the coating layers from the fracture zone during the preparation of the samples for analyses. The thickness of the coating layer also appeared to be less for CF1 than for other coatings (approx. 50 µm for CF1 and between 90 and 120 µm for CF2, CF3 and CF11).

The differences in the adhesion strength between the samples can be explained by the penetration of the coatings into the wood structure. Adhesion of a coating to a substrate occurs via two main mechanisms: mechanical anchoring and chemical interactions. Chemical interactions include adsorption and chemisorption with the formation of chemical bonds as well as electrostatic interactions at the interface between the substrate and the coating [22,28]. Mechanical adhesion results from penetration and hardening of the coating

into the substrate. Wood is a porous material and therefore, mechanical adhesion generally plays an important role in the adhesion of paints and adhesives onto wood. Chemicals migrate into the wood structure by capillary permeation through open porosity and the phenomenon is modulated by parameters such as the size and shape of the chemical, or the nature of the solvent. It was reported that water-based coatings are prone to penetrate wood to a lesser extent and exhibited lower adhesion strengths than organic solvent-based ones [22,29]. The absorption of water or solvent from the coating by the wood surface changes the flow properties such as viscosity, solid content, and dispersion (particulate agglomerations). The penetration of the coating components into the wood was investigated using EDAX. Potassium was observed at depths down to around 200 µm, whereas silicon was detected only down to 50–100 µm. Potassium ions and probably hydroxide ions are the most water-transportable coating species due to their reduced geometric dimensions. Silicon is present in the coatings in various species ranging from simple silicate monomers to oligomer components with low mobility; a decrease of silicate modulus generally reduces the size of silicates species and hence increases their penetration into substrates. The contribution of penetration to adhesion was attributed to a few micrometers of hardened coatings at the interface between wood and coating layer. Alkaline metal silicates introduced into wood need additional presence of a curing agent (an acid or polyvalent metal cations such as Ca^{2+}, Zn^{2+}, Al^{3+}) to polymerize and form insoluble and mechanically resistant materials [30,31]. The usefulness of the penetration of silicates for adhesion is influenced by the penetration of other chemicals such as calcium carbonate or zinc oxide that could act as curing agents. The lower adhesion strengths measured with some coating formulations were attributed to lower ingress of such solid particles into the wood. It was observed that the application of water glass alone at the surface of wood before coating failed in increasing the adhesion, and even worse adhesion was measured in certain cases (results not shown).

Typical viscosities as a function of shear rate curves of potassium water glass, lithium water glass, and some coating formulations are shown in Figure 3.

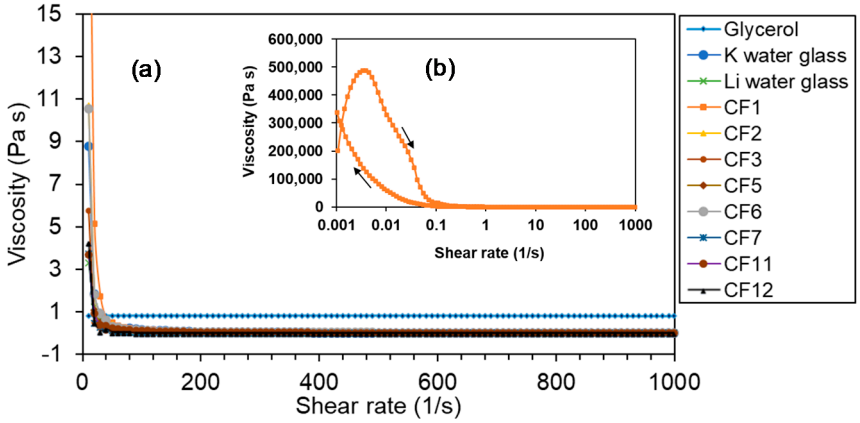

Figure 3. (**a**) Viscosity as a function of shear rate for selected formulations and (**b**) a typical flow behavior at lower shear rates (CF1).

The flow curves of water glasses and the coatings exhibited a shear thinning profile characteristic for suspensions, such as heterogeneous dispersion paints [32,33]. Only glycerol showed a Newtonian profile. In general, dispersed solid particles agglomerate and form a network that hinders random movements, the increase of the shear rate breaks the microstructure and thus decreases the viscosity, while the constraint against the particle flow decreases. The flow response of water glass is complex and can range from Newtonian to complex shear thickening. It changes with solid content, modulus, and the presence of impurities like metal salts [34–36]. A suspension-like model was proposed for sodium water glass in which monomeric and small oligomeric silicate species act as binders, whereas large oligomeric colloidal particles and small metallic cations act as effective rigid

particles [35]. However, the microstructure was easily destroyed, resulting in a rapid drop of viscosity with an increase of the shear rate. The formulations showed a high viscosity at lower shear rate and a very low viscosity at high shear rate, between 0.016 Pa s and 0.25 Pa s at 100 to 200 s^{-1} estimated as the shear rate range generated by paint brushing on a substrate [37]. The flow curve measured by increasing (forward measurement) or decreasing (backward measurement) the shear rate for CF1 shown in Figure 3b, exhibited a typical flow behavior of the formulations at lower shear rates. The high viscosity suggests a steady equilibrium shear reversible gel-like structure at rest with weak interactions between particles. A detailed description of the rheological properties of the coatings at low shear rates and relation with properties such as leveling, sagging and sedimentation requires further extensive analyses, and that is beyond the scope of this research. The increase of the viscosity after coating application, the size and dispersion of particles and the settling properties could prevent penetration for some coatings. An increase of the solid content or addition of glycerol or sugar compounds are susceptible to cause the aggregation of particles. Glycerol is known as a coalescent additive. Low adhesion values were also measured when glycerol was substituted by the same amount of polyglycerol samples obtained by polymerization of glycerol catalyzed by lithium hydroxide at 240 °C for 6 h (results not shown). Large particles probably originating from aggregation can be seen in the micrographs (e.g., CF2, CF3 and CF11). However, For CF11, a more uniform interface was observed as compared to other coatings without signs of debonding or deposition of the coatings.

A relatively high amount of silicon was noticed in wood with CF3 (with sucrose additive) and was attributed to the ability of sugar to depolymerize and bond silicates in more soluble compounds. The formation of soluble organo-silicate complexes has been demonstrated in the literature for certain sugars including xylose [38]. The depolymerization of silicates by xylose could reduce or delay their contribution to the hardening process and explains the lower adhesion strength and performances measured with this sugar additive (CF4). The better adhesion with dextrin could be due to its contribution as a binding polymeric material able to adhere to some extent at the wood surface.

3.3. ATR-FTIR Analyses

ATR-FTIR analyses were performed on water glass, fresh coating formulations, and coatings after two weeks of curing. The spectra obtained with CF1 and CF12 are displayed in Figure 4. The spectra obtained with other samples were showing the same results (spectra not shown).

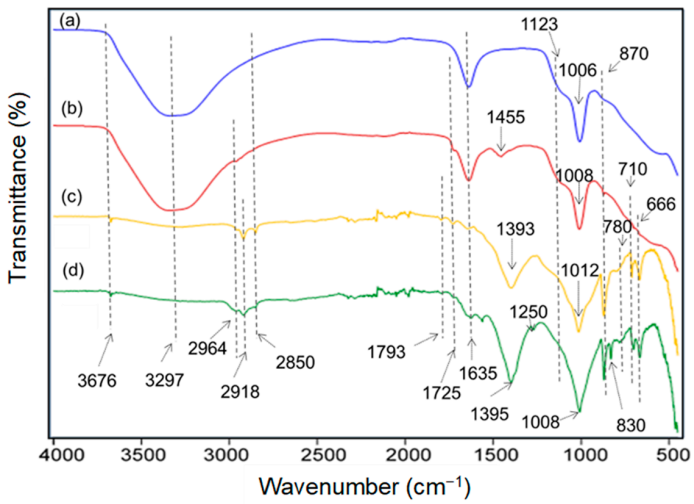

Figure 4. ATR-FTIR spectra of (**a**) potassium water glass (**b**) fresh liquid CF1 (**c**) hardened CF1 and (**d**) hardened CF12.

The vibration bands and corresponding functional groups are summarized in Table 3.

Table 3. FTIR spectra vibration bands assignments [39–45].

Bands	Assignments
3676 cm^{-1}	Stretching of isolated and mutually hydrogen bonded- Si–OH and Mg–OH
3297 cm^{-1}	Stretching O–H in water and silanol SiO–H hydrogen bonded- with water
2935, 2918, 2850 cm^{-1}	Asymmetric and symmetric stretching of C–H in methylene and methyl groups
1793, 1725 cm^{-1}	C=O carbonyls (CO_3^{2-} and carbonyl in acrylic resins
1635 cm^{-1}	Bending vibration of water (H–O–H)
1455, 1393 cm^{-1}	Asymmetric stretching of CO_3^{2-}
1120 cm^{-1}	Asymmetric Stretching of Si–O–Si in highly cross-liked zone, e.g., (Si–O)4 closed cage
1012, 1008, 1006 cm^{-1}	Asymmetric stretching of Si–O in short siloxane-chain
872 cm^{-1}	Out of plane bending (CO_3^{2-}), symmetric stretching Si–O
780 cm^{-1}	–CH_3 rocking and Si–C wagging stretching in Si–CH_3
710 cm^{-1}	In plane bending (CO_3^{2-})
666 cm^{-1}	Stretching of Si–O–Si in tetrahedral unit, stretching of Si–O–Mg

The band at 3673 cm^{-1} can be attributed to stretching of Si–OH hydroxyl of silanol groups of mutually H-bonded silicate compounds as well as to Mg–OH stretching in Talc. The broad band centered at 3297 cm^{-1} showed contribution of hydroxyl groups of adsorbed water and water in pores of the materials and stretching of Si–OH silanols H-bonded to water molecules. This band was very large for water glass and the fresh coating formulation because of their high-water content and overlapping with vibration bands of other functional groups (Si–OH and Mg–OH). The presence of water can also be seen from the bending vibration band at 1637 cm^{-1} occurring in molecular water. The bands at 2925, 2918 and 2850 cm^{-1} generally resulting from symmetric and asymmetric stretching of C–H were attributed to the presence of acrylic-styrene resins, glycerol, or others organic additives. Styrene-acrylic resins and carbonate groups (CO_3^{2-}) contributed to stretching bands at 1793 and 1725 cm^{-1} assigned to carbonyl (C=O) groups. The bands observed at 1393, 872 and 713 cm^{-1} were assigned to asymmetric stretching, out of plane bending and in-plane bending in carbonate compounds, respectively [42]. The domain between 1200 and 800 cm^{-1} displayed asymmetric and symmetric stretching of Si–O and the positions of bands revealed the degree of cross-linking of silicate species and association with metallic species (e.g., calcium ions) in metal silicates compounds. The main stretching band of Si–O–Si bonds appeared between 1090 and 1080 cm^{-1} in amorphous pure silica [40,46]. This vibration band is shifted towards lower wavenumbers around 1010 cm^{-1} or less for stretching of species such as $SiO(OH)_3^-$ (Q1) and $SiO_2(OH)_2^{2-}$ (Q2) groups as observed in the spectra of water glass and of fresh coatings. The stretching of Si–O in isolated SiO_4^{4-} (Q0) can be found down to approximately 850 cm^{-1} [39]. The combination of silicates with metal species such as calcium ions or zinc ions in calcium silicate or zinc silicate compounds reduced the interconnection between silicates and polymerization degree of the chains, while also shifting the vibrations bands of Si–O–Si towards lower wavenumbers. For example, the stretching of Si–O–Si was observed around 970 cm^{-1} in calcium silicates when the proportion of calcium ions incorporated in the structure increased [44]. The fact that the maximum absorption of the shoulder band in the Si–O region appeared at 1012–1008 cm^{-1} for the coatings suggested a curing mechanism involving preferably reaction of silicates with calcium, zinc or magnesium species from calcium carbonate, zinc oxide and talc additives instead of formation of silica networks. The results are in agreement with X-ray diffraction (XRD) analyses reported by Kazmina et al. [10] for similar systems. Curing of silicates can also occur naturally by reaction with carbon dioxide of the environ-

ment. Carbon dioxide diffuses inside the material and is dissolved in the pore solution and forms carbonic acid that neutralizes the alkalinity and leads to the occurrence of silicate polymerization. The dissolution of zinc oxide, calcium carbonate, or liberation of metal cations or ions into pore solutions and the reaction of silicates with surface metallic species yield to calcium silicates, zinc silicates and bonding of the particles.

3.4. Influence of Wood Mineralization

Mineralization was performed under mild conditions to allow mainly modification at the wood surface. The weight percent gain of wood determined as percentage of mass increase of the samples after the double impregnation processes were between 2% and 3% (values measured without leaching). The coating performances of formulation CF7 applied onto modified wood samples are shown in Table 4.

Table 4. Coating performances of CF7 on pre-mineralized wood samples (MW1 and MW2 wood mineralized with potassium water glass, and then boric acid or sodium bicarbonate, respectively).

Pre-Mineralized Wood	Pull-off Adhesion Strength (MPa) #	Assessment of the Cross-Cut Test	Scratch Resistance (N)	Assessment of the Impact Test (400 mm) *
MW1	3.8 (0.26)	1	6	3.5 (6.4)
MW2	2.6 (0.18)	1	5.5	3.5 (6.8)

Standard deviation is in the parentheses. * 400 mm is the drop height and values in parentheses the diameter of the crater caused by impact.

The results showed an increase of the adhesion strength after mineralization of wood. A considerable increase was observed for wood mineralized with potassium water glass and cured with boric acid, from 2.2 MPa on untreated wood to 3.8 MPa on pretreated wood. The silicification of wood by a double treatment with boric acid curing has been reported as one of the best methods to produce insoluble silica in wood [14,15]. Chemical reactions between silicate species in the coatings and silica at the wood surface could contribute to an increase of the adhesion of coatings. Low adhesion was measured when potassium water glass was applied alone (result not shown) without a second curing treatment. The results showed that adhesion between silicate coatings and wood can be significantly improved by using pre-mineralized wood. These results are in agreement with commercial offers using mineralized alkyds or drying oils primers.

3.5. Water Resistance of the Samples

Liquid water absorptions expressed as the increase of mass per surface area of coating exposed to water (kg/m^2) are shown in Figure 5 for selected (based on adhesion strength values) coatings.

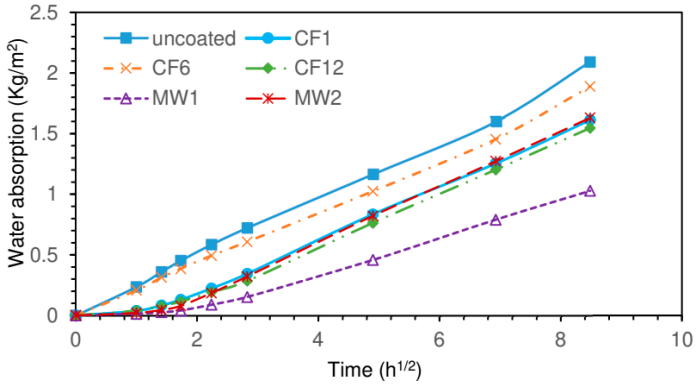

Figure 5. Water absorption of uncoated wood and coated wood (CF1, CF6, CF12, MW1 and MW2).

Water absorption was slightly reduced by most of the coatings. The lowest water uptake was measured for MW1. The samples (CF1, CF12, MW1 and MW2) showed low

water absorption during the first two hours in water, but after the amount of water uptake increased considerably. Water absorption was not reduced by the addition of methyl siliconate. The results could be due to the method used for the application. The application was carried out by one single pass that led to craters and pores allowing for water transport as observed in confocal microscopy analyses of the coating surfaces (Figure 6).

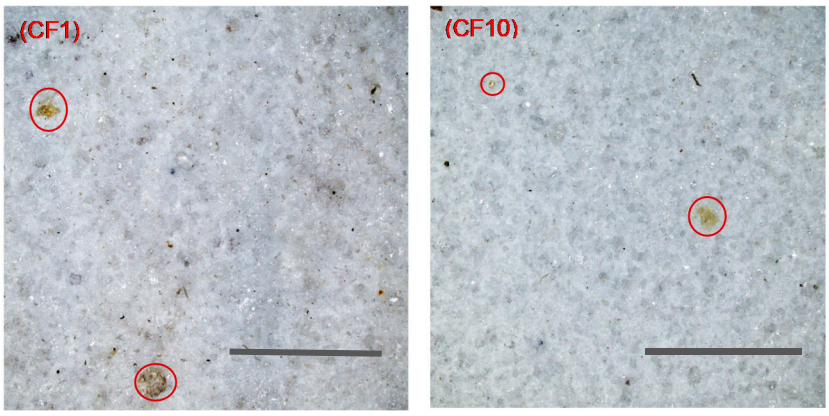

Figure 6. Confocal microscopy images of the surfaces of CF1 and CF10 (magnification 5×, scale bars represent 1 mm).

These coatings are not film-forming materials and a multi-layer application could be useful to reduce the formation of such open porosity. The dissolution of soluble components (e.g., potassium salts) could exacerbate the water permeability. It is important to note that cracks were observed at some coatings after 24 h in water, especially at coatings with low adhesion. Cracking and debonding increased while drying the samples, which resulted from the dimensional instability of wood. A picture of a coating sample with one of the highest surface damages (CF6) due to moisture (soaking in water for five days and indoor air drying for height weeks) is shown in Figure 7. The samples with higher adhesion strength values were less degraded by water as can be seen with CF1.

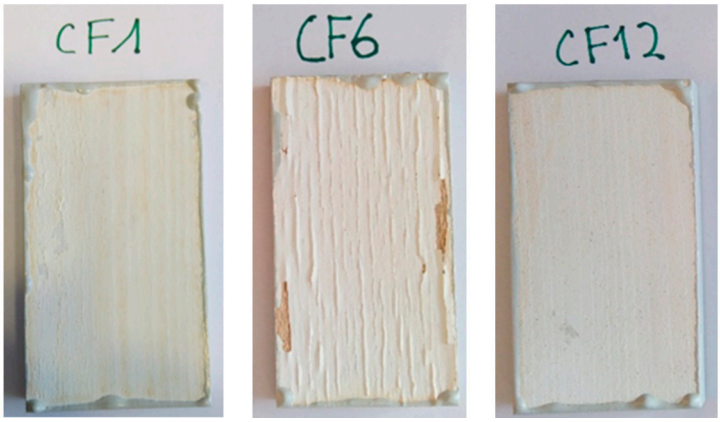

Figure 7. Photographs of CF1, CF6 and CF12 soaked in liquid water for 5 days and exposed for drying to ambient indoor conditions (temperature (23 ± 3) °C and (50 ± 5)% relative humidity) for eight (08) weeks.

No signs of cracks were noticed on the sample with methyl siliconate (CF12); only some discoloration appeared and was attributed to wood extractives. Silicate modified with organoalkoxysilanes showed an increase in flexibility as reported for the decrease of modulus of elasticity of organically-modified silicates on steel [47]. The increase of flexibility could explain the resistance of the coatings to the formation of cracks despite high water absorption. The surface of this coating was not chalking after residence in water as

opposed to other coating formulations. Optimization of the formulations to the reduced water absorption is under progress (results will be shown elsewhere).

4. Conclusions

Various silicate-based formulations were prepared and applied on wood to study the coating performances (adhesion, scratch and impact resistance, and water resistance). The adhesion mechanism was found to be dependent on mechanical anchoring for untreated wood and related to penetration of the coatings into the wood. Poor adhesion strength (<2 MPa) to adhesion acceptable for coatings (2.5–2.70 MPa) were measured depending on the formulations. The surface pre-mineralization of wood increased the adhesion strength by increasing chemical bonding. An increase of the adhesion to 3.8 MPa was obtained for wood pretreated with a double impregnation of potassium silicate and boric acid solutions. An addition of polyols (glycerol, sucrose or D-xylose) was not effective in improving the coatings' properties. The coatings showed acceptable scratch and impact resistances, but the formulations must be improved to increase water resistance. Substitution of a part of potassium water glass by potassium methyl siliconate improved the resistance to crack formation without significant changes of the other performances of the coatings.

Author Contributions: Conceptualization and methodology, A.M.C.Y.; analyses, A.M.C.Y. and J.Ž.; writing—original draft, A.M.C.Y.; review and editing, A.M.C.Y., J.Ž., S.D., and M.P.; supervision, M.P.; funding acquisition A.M.C.Y. and M.P. All authors have read and agreed to the published version of the manuscript.

Funding: This research was funded by the Slovenian National Research Agency (ARRS) ("SilWood-Coat" N4-0117 and "Wood and lignocellulosic composites" P4-0015).

Data Availability Statement: The raw data presented in this study are available on request from the corresponding author.

Acknowledgments: The authors are grateful to Angela Balzano for her technical assistance in SEM-EDAX analyses.

Conflicts of Interest: The authors declare no conflict of interest.

References

1. Popescu, C.-M.; Pfriem, A. Treatments and modification to improve the reaction to fire of wood and wood based products—An overview. *Fire Mater.* **2020**, *44*, 100–111. [CrossRef]
2. Borges, C.C.; Denzin, T.G.H.; Moreira, C.T.; Duarte, P.J.; Junqueira, T.A. Nanoparticles-based wood preservatives: The next generation of wood protection? *CERNE* **2018**, *24*, 397–407. [CrossRef]
3. Bao, W.; Zhang, M.; Jia, Z.; Jiao, Y.; Cai, L.; Liang, D.; Li, J. Cu thin films on wood surface for robust superhydrophobicity by magnetron sputtering treatment with perfluorocarboxylic acid. *Eur. J. Wood Prod.* **2019**, *77*, 115–123. [CrossRef]
4. Köhler, R.; Sauerbier, P.; Ohms, G.; Viöl, W.; Militz, H. Wood protection through plasma powder deposition—An alternative coating process. *Forests* **2019**, *10*, 898. [CrossRef]
5. Parashar, G.; Bajpayee, M.; Kamani, P.K. Water-borne, non-toxic, high-performance inorganic silicate coatings. *Surf. Coat. Int. B* **2003**, *86*, 209–216. [CrossRef]
6. Pal, S.; Contaldi, V.; Licciulli, A.; Marzo, F. Self-cleaning mineral paint for application in architectural heritage. *Coatings* **2016**, *6*, 48. [CrossRef]
7. Loganina, V.I. Polymer silicate paints for interior decorating. *Contemp. Eng. Sci.* **2015**, *8*, 171–177. [CrossRef]
8. Fraci, A.T. *Waterborne Silicates in Coatings and Construction Chemicals in Inorganic Zinc Coatings, History, Chemistry, Properties, Applications and Alternatives*, 2nd ed.; Francis, R.A., Ed.; The Australasian Corrosion Association Inc.: Victoria, Australia, 2013; pp. 227–258.
9. Kumar, S.P.; Takamori, S.; Arakia, H.; Kuroda, S. Flame retardancy of clay–sodium silicate composite coatings on wood for construction purposes. *RSC Adv.* **2015**, *5*, 34109–34116. [CrossRef]
10. Kazmina, O.; Lebedeva, E.; Mitina, N.; Kuzmenko, A. Fire-proof silicate coatings with magnesium-containing fire retardant. *J. Coat. Technol. Res.* **2018**, *15*, 543–554. [CrossRef]
11. Ramasamy, S.; Hussin, K.; Al Bakri, M.M.A.; Ghazali, C.M.R.; Sandhu, A.V.; Binhussain, M.; Shahedan, N.F. Adhesiveness of kaolin based coating material on lumber wood. *Key Eng. Mater.* **2016**, *673*, 47–54. [CrossRef]
12. Ramasamy, S.; Al Bakri Abdullah, M.M.; Kamarudin, H.; Yue, H.; Jin, W. Improvement of kaolin based geopolymer coated wood substrates for use in NaOH molarity. *Mater. Sci. Forum* **2019**, *967*, 241–249. [CrossRef]

13. Shaikh, F.U.A.; Haque, S.; Sanjayan, J. Behavior of fly ash geopolymer as fire resistant coating for timber. *J. Sustain. Cem. Based Mater.* **2018**, *8*, 1–16. [CrossRef]
14. Standard ISO 4624. Paints and Varnishes-Pull Off Test for Adhesion. 2016. Available online: https://www.iso.org/standard/62351.html (accessed on 5 January 2021).
15. Standard EN ISO 2409. Paints and Varnishes-Cross Cut Test. 1997. Available online: https://www.iso.org/standard/76041.html (accessed on 5 January 2021).
16. Standard EN ISO 1518-1: 2000 Paint and Varnishes-Scratch Test. Available online: https://standards.iteh.ai/catalog/standards/cen/a2ff84bf-9c58-4b9e-a651-4c3899ae56fa/en-iso-1518-2000 (accessed on 5 January 2021).
17. Standard ISO 4211-4. Furniture-Tests for Surfaces-Assessment of Resistance to Impact. 1995. Available online: https://standards.iteh.ai/catalog/standards/sist/44c7b7b9-ec61-485e-8909-6e317e0e9f72/sist-iso-4211-4-1995 (accessed on 5 January 2021).
18. Chen, G.C. Treatment of wood with polysilicic acid derived from sodium silicate for fungal decay protection. *Wood Fiber Sci.* **2009**, *410*, 220–228.
19. Furuno, T.; Shimada, K.; Uehara, T.; Jodai, S. Combinations of wood and silicate II. Wood-mineral composites using water glass and reactants of barium chloride, boric acid, and borax, and their properties. *Mokuzai Gakkaishi* **1992**, *38*, 448–457.
20. Thougaard, L.; Hayden, J.P. Wood Preservation Method Using Sodium Silicate and Sodium Bicarbonate, WO 2014/101979 A2. Available online: https://patents.google.com/patent/WO2014101979A2/en (accessed on 5 January 2021).
21. EN 927-5:2006—Paints and Varnishes—Coating Materials and Coating Systems for Exterior Wood—Part 5: Assessment of the Liquid Water Permeability. Available online: https://www.en-standard.eu/csn-en-927-5-paints-and-varnishes-coating-materials-and-coating-systems-for-exterior-wood-part-5-assessment-of-the-liquid-water-permeability/ (accessed on 5 January 2021).
22. Meijer, M.D. *A review of interfacial aspects in wood coatings: Wetting, surface energy, substrate penetration and adhesion. COST E18 Final Seminar*; European Cooperation in Science and Technology: Brussels, Belgium, 2005.
23. Sonmez, A.; Budakci, M.; Bayram, M. Effect of wood moisture content on adhesion of varnish coatings. *Sci. Res. Essays* **2009**, *4*, 1432–1437.
24. Kesik, H.I.; Akyildiz, M.H. Effect of the heat treatment on the adhesion strength of water based wood varnishes. *Wood Res.* **2015**, *60*, 987–994.
25. Hazir, E.; Koc, K.H. Evaluation of wood surface coating performance using water based, solvent based and powder coating. *Maderas. Cienc. Tecnol.* **2019**, *21*, 467–480. [CrossRef]
26. Oblak, L.; Kričej, B.; Lipušček, I. The comparison of the coating systems according to the basis criteria. *Wood Res.* **2006**, *51*, 77–86.
27. Çakıcıer, N.; Korkut, S.; Korkut, D.S. Varnish layer hardness, scratch resistance, and glossiness of various wood species as affected by heat treatment. *BioResources* **2011**, *6*, 1648–1658.
28. Ahola, P. Adhesion between paints and wooden substrates: Effects of pre-treatments and weathering of wood. *Mater. Struct.* **1995**, *28*, 350–356. [CrossRef]
29. De Meijer, M.; Van de Velde, B.; Militz, H. Rheological approach to the capillary penetration of coating into wood. *J. Coat. Technol.* **2001**, *73*, 39. [CrossRef]
30. Furuno, T.; Uehara, T.; Jodai, S. Combinations of wood and silicate I. Impregnation by water glass and applications of aluminum sulfate and calcium chloride as reactants. *Mokuzai Gakkaishi* **1991**, *37*, 462–472.
31. Pereyra, A.M.; Giudice, C.A. Flame-retardant impregnants for woods based on alkaline silicates. *Fire Saf. J.* **2009**, *44*, 497–503. [CrossRef]
32. Arora, S.; Laha, A.; Majumdar, A.; Butola, B.S. Prediction of rheology of shear thickening fluids using phenomenological and artificial neural network models. *Korea Aust. Rheol. J.* **2017**, *29*, 185–193. [CrossRef]
33. Ge, J.; Tan, Z.; Li, W.; Zhang, H. The rheological properties of shear thickening fluid reinforced with SiC nanowires. *Results Phys.* **2017**, *7*, 3369–3372. [CrossRef]
34. Yang, Q.; Yang, X.H.; Wang, P.; Zhu, W.L.; Chen, X.Y. The viscosity properties of zinc-rich coatings from sodium silicate solution modified with aluminium chloride. *Pigment Resin Technol.* **2009**, *38*, 153–158. [CrossRef]
35. Yang, X.; Zhu, W.; Yang, Q. The viscosity properties of sodium silicate solutions. *J. Solut. Chem.* **2008**, *37*, 73–83. [CrossRef]
36. Yang, X.; Zhang, S. Characterizing and modeling the rheological performances of potassium silicate solutions. *J. Solution Chem.* **2016**, *45*, 1890–1901. [CrossRef]
37. Fischer, E.K. Rheological properties of commercial paints. *J. Colloid Sci.* **1950**, *5*, 271–281. [CrossRef]
38. Lambert, J.B.; Lu, G.; Singer, S.R.; Kolb, V.M. Silicate complexes of sugars in aqueous solution. *J. Am. Chem. Soc.* **2004**, *126*, 9611–9625. [CrossRef]
39. Bobrowski, A.; Stypuła, B.; Hutera, B.; Kmita, A.; Drożyński, D.; Starowicz, M. FTIR spectroscopy of water glass—The binder moulding modified by ZnO nanoparticles. *Metalurgija* **2012**, *51*, 477–480.
40. Khan, A.S.; Khalid, H.; Sarfraz, Z.; Khan, M.; Iqbal, J.; Muhammad, N.; Fareed, M.A.; Rehman, I.U. Vibrational spectroscopy of selective dental restorative materials. *Appl. Spectrosc. Rev.* **2016**. [CrossRef]
41. Al-Oweini, R.; El-Rassy, H. Synthesis and characterization by FTIR spectroscopy of silica aerogels prepared using several $Si(OR)_4$ and $R00Si(OR')_3$ precursors. *J. Mol. Struct.* **2009**, *919*, 140–145. [CrossRef]
42. Cai, G.-B.; Chen, S.-F.; Liu, L.; Jiang, J.; Yao, H.-B.; Xu, A.-W.; Yu, S.-H. 1,3-Diamino-2-hydroxypropane-N, N, N′, N′-tetraacetic acid stabilized amorphous calcium carbonate: Nucleation, transformation and crystal growth. *Cryst. Eng. Comm.* **2010**, *12*, 234–241. [CrossRef]

43. Ferrage, E.; Martin, F.; Petit, S.; Pejo-Soucaille, S.; Micoud, P.; Fourty, G.; Ferret, J.; Salvi, S.; De Parseval, P.; Fortune, J.P. Evaluation of talc morphology using FTIR and H/D substitution. *Clay Miner.* **2003**, *38*, 141–150. [CrossRef]
44. Giraudo, N.; Bergdolt, S.; Wohlgemuth, J.; Welle, A.; Schuhmann, R.; Königer, F.; Thissen, P. Calcium Silicate Phases Explained by High-Temperature-Resistant Phosphate Probe Molecules. *Langmuir* **2016**, *32*, 13577–13584. [CrossRef]
45. Maddalena, R.; Hall, C.; Hamilton, A. Effect of silica particle size on the formation of calcium silicate hydrate [C-S-H] using thermal analysis. *Thermochim. Acta* **2019**, *672*, 142–149. [CrossRef]
46. Li, K.-M.; Jiang, J.-G.; Tian, S.-C.; Chen, X.-J.; Yan, F. Influence of silica types on synthesis and performance of amine−silica hybrid materials used for CO_2 capture. *J. Phys. Chem. C* **2014**, *118*, 2454–2462. [CrossRef]
47. Latella, B.A.; Ignat, M.; Barbe, C.J.; Cassidy, D.J.; Bartlett, J.R. Adhesion behaviour of organically-modified silicate coatings on stainless steel. *J. Sol Gel Sci. Technol.* **2003**, *26*, 765–770. [CrossRef]